Immunity, Volume *39*

Supplemental Information

Control of T Helper 2 Responses by Transcription Factor IRF4-Dependent Dendritic Cells

Yan Gao, Simone A. Nish, Ruoyi Jiang, Lin Hou, Paula Licona-Limón, Jason S. Weinstein, Hongyu Zhao, and Ruslan Medzhitov

Supplemental Inventory

Supplemental Figures and Tables

Supplementary Figure 1

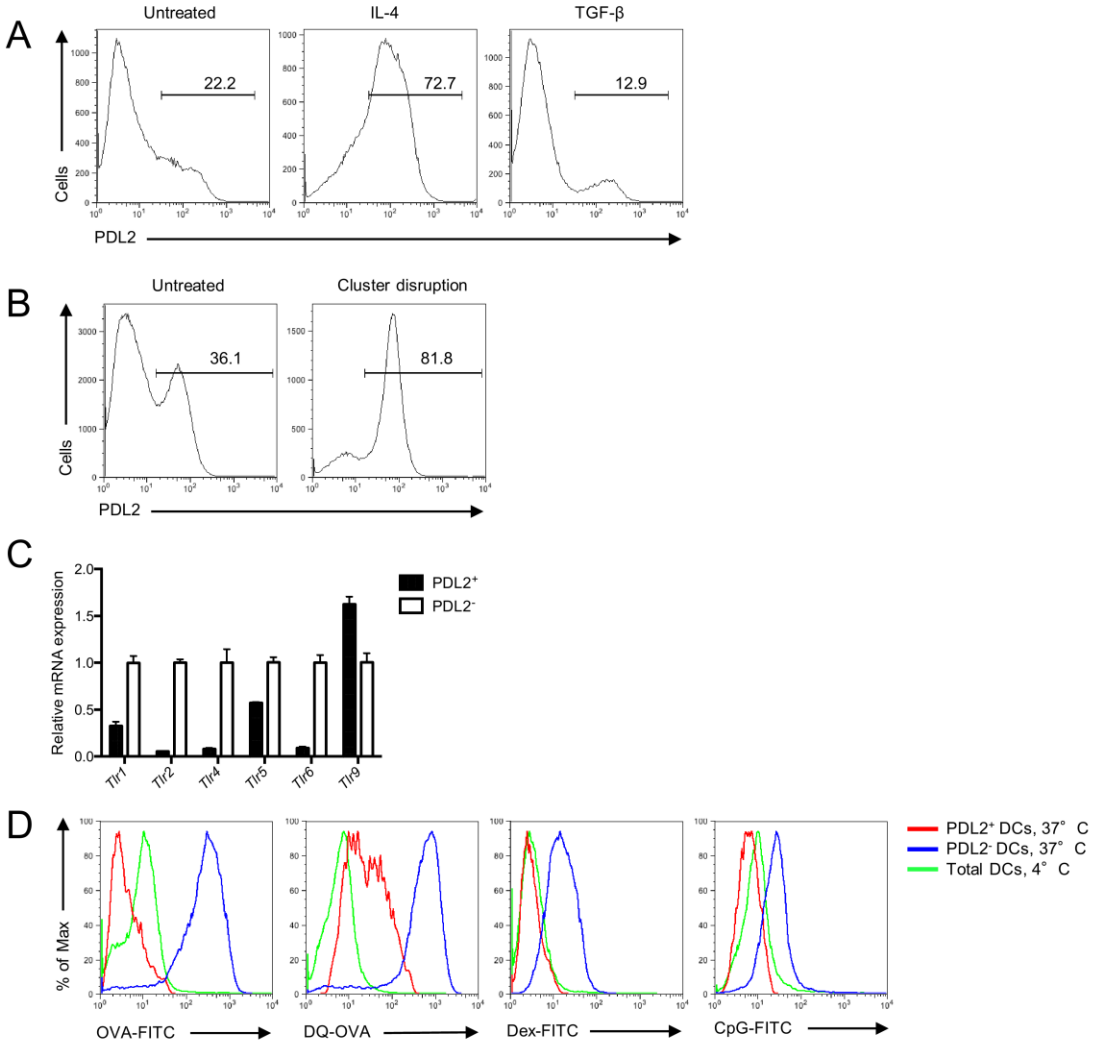

Figure S1. Characterization of PDL2$^+$ BMDCs, Related to Figure 1

(A) Regulation of PDL2$^+$ BMDC differentiation by IL-4 and TGF-β treatment. IL-4 (100 ng/ml) and TGF-β (10 ng/ml) were added to BMDC cultures for the last 48hrs of the 6-day culture. Percentages of PDL2$^+$ BMDCs were analyzed on day 6 by flow cytometry. Plots are gated on CD11c$^+$ cells. Data are representative of three independent experiments.

(B) PDL2$^+$ BMDC differentiation induced by disruption of E-cadherin-mediated adhesion. BMDC clusters on day 5 were physically disrupted by passing through magnetic columns (Jiang et al, 2009) and remained in culture for 24hrs. Percentages of PDL2$^+$ BMDCs were analyzed on day 6 by flow cytometry. Plots are gated on CD11c$^+$ cells. Data are representative of three independent experiments.

(C) TLR mRNA expression analyzed by real-time RT-PCR in PDL2$^+$ and PDL2$^-$ BMDCs sorted from bone marrow cultures. Expression values of PDL2$^-$ DCs were set as calibrator. Data are representative of three independent experiments and bar graphs show mean ± SD.

(D) Uptake of OVA-FITC, DQ-OVA, Dextran (Dex)-FITC and CpG-FITC by PDL2$^+$ and PDL2$^-$ BMDCs. Total BMDCs were incubated with the indicated fluorescently labeled antigens *in vitro* for 20 minutes at 37°C or 4°C. Data are representative of two independent experiments.

Supplementary Figure 2

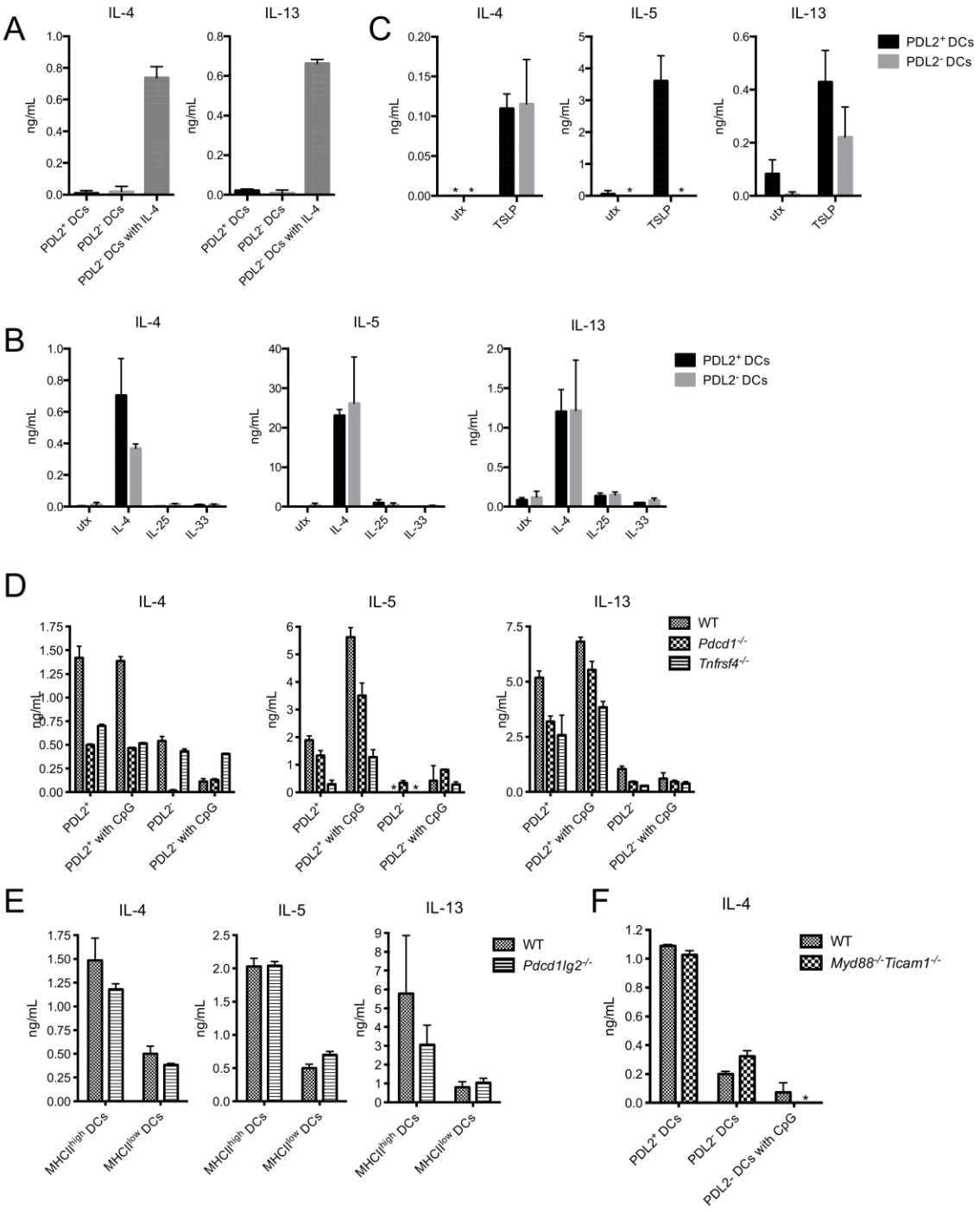

Figure S2. Characterization of the Th2 Response Induced by PDL2^{+} BMDCs, Related to Figure 2

(A) Sorted PDL2^{+} and PDL2^{-} BMDCs were cultured together with naïve OT-II T cells *in vitro* in the presence of OVA peptide (amino acids 323-339). IL-4 was added where indicated. Supernatants from day 4 co-cultures were collected, and IL-4 and IL-13 amounts were measured by ELISA. Data are representative of three independent experiments and bar graphs show mean ± SD.

(B and C) Sorted PDL2^{+} and PDL2^{-} BMDCs were cultured together with WT splenic naïve CD4 T cells (CD44^{low}CD62L^{hi}) for 4 days with α-CD3 stimulation. IL-4, IL-25 or IL-33 (B) and TSLP (C) were added where indicated. Supernatants from day 4 co-cultures were assessed for IL-4, IL-5 and IL-13 production. Data are representative of at least two independent experiments and bar graphs show mean ± SD.

(D) Splenic CD44^{hi}CD62L^{low} effector or memory CD4+ T cells from WT, *Pdcd1*$^{-/-}$ or *Tnfrsf4*$^{-/-}$ mice were cultured with PDL2^{+} or PDL2^{-} BMDCs in the presence or absence of CpG DNA and were examined for Th2 responses. Data are representative of at least three independent experiments and bar graphs show mean ± SD.

(E) Effector or memory Th2 response induced by MHCII^{hi} and MHCII^{low} BMDCs from WT or *Pdcd1lg2*$^{-/-}$ mice. Data are represented as mean ± SD.

(F) IL-4 production by effector or memory CD4 T cells stimulated with BMDC subsets from WT or *Myd88*$^{-/-}$*Ticam1*$^{-/-}$ mice. Data are represented as mean ± SD.

Supplementary Figure 3

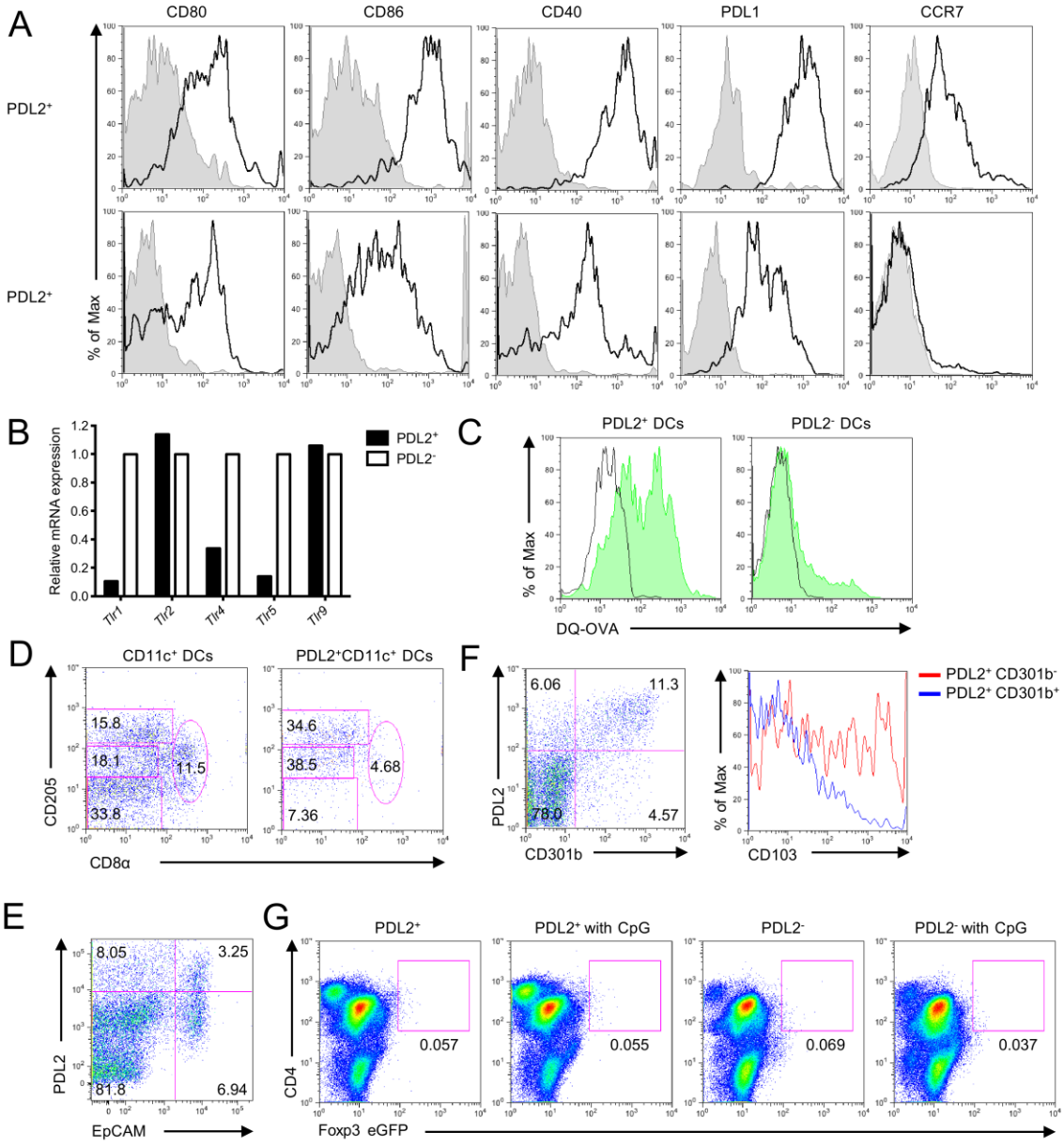

Figure S3. Characterization of PDL2$^+$ DCs in the Skin Draining Lymph Nodes, Related to Figure 3

(A) Surface phenotyping of PDL2$^+$ and PDL2$^-$ skin dLN DCs (CD80, CD86, CD40, PDL1 and CCR7). Shaded histogram indicates isotype control.

(B) TLR mRNA expression was analyzed by real-time RT-PCR in PDL2$^+$ and PDL2$^-$ skin dLN DCs. Expression values of PDL2$^-$ DCs were set as calibrator.

(C) Uptake and processing of subcutaneously injected DQ-OVA antigen by PDL2$^+$ or PDL2$^-$ skin dLN DCs. Mice were immunized subcutaneously in the rear footpads with 50μg DQ-OVA in PBS. Popliteal draining lymph node cells were examined by flow cytometry 24 hours after immunization. Data are representative of two independent experiments.

(D) Composition of PDL2+ DCs in skin dLNs. Lymphocytes from skin dLNs were examined by flow cytometry for CD11c, PDL2, CD8α and CD205 expression. Gating strategy for identification of Langerhans cells (LCs), dermal DCs, CD8α DCs and double negative (DN) DCs was stated in the main text.

(E) Co-staining of PDL2 and EpCAM on skin dLN CD11c$^+$ DCs.

(F) Co-staining of PDL2, CD301b and CD103 on skin dLN CD11c$^+$ DCs.

(G) Splenic CD4+ T cells from Foxp3-eGFP mice were co-cultured with sorted PDL2$^+$ and PDL2$^-$ DCs from skin dLNs. CpG was added to co-culture where indicated. Foxp3-eGFP expression was analyzed by flow cytometry on day 4. Data are representative of at least three independent experiments.

Supplementary Figure 4

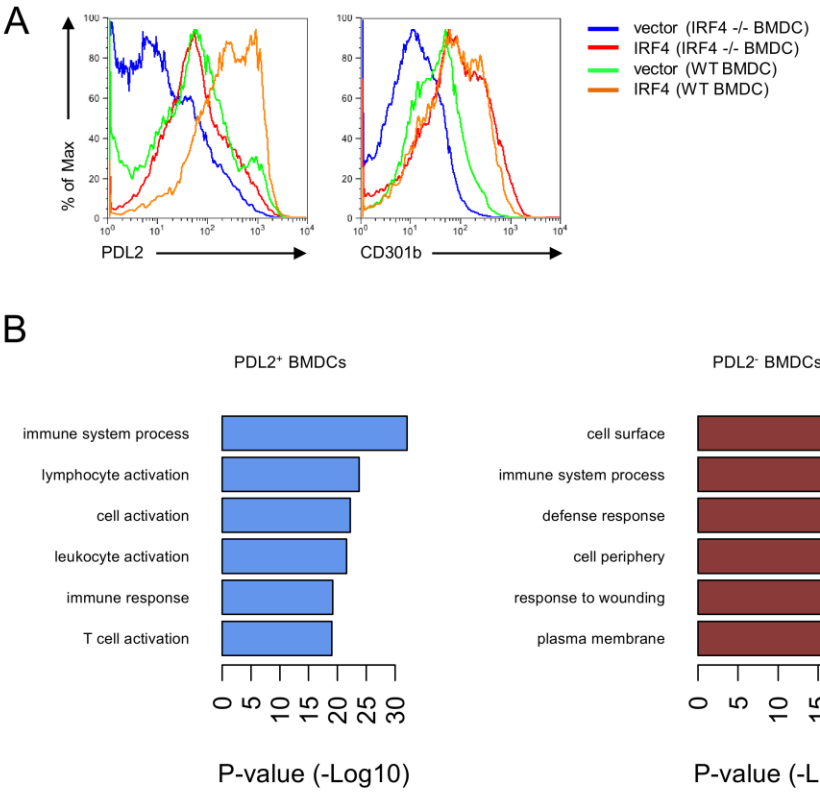

Figure S4. The Role of IRF4 in PDL2^{+} DCs, Related to Figure 4

(A) Reconstitution of IRF4 in *Irf4*$^{-/-}$ BMDCs. WT and *Irf4*$^{-/-}$ BMDCs were retrovirally transduced with an IRF4 construct, and the surface expression of PDL2 and CD301b was examined by flow cytometry at day 5.

(B) Gene Ontology analysis was performed for genes with PC2 scores greater than an absolute designated threshold of ±1.00 as determined by RNA-Seq analysis. The top six overrepresented GO functional identifiers associated with PDL2^{+} and PDL2^{-} BMDC populations are displayed in terms of their Log10 p-values.

(C and D) mRNA expression of the AP-1 family (C) and Ets family (D) transcription factors was analyzed by real-time RT-PCR in PDL2^{+} and PDL2^{-} BMDCs. Expression values of PDL2^{-} BMDCs were set as calibrator.